Indian Journal of Geo-Marine Sciences
Vol. 41(1), February 2012, pp. 45-55

Artificial neural networks for estimation of temporal rate coefficient of equilibrium bar volume

Murat Kankal[1*], Murat İhsan Kömürcü[1], Ömer Yüksek[1] & Adem Akpınar[1,2]

[1] Karadeniz Technical University, Civil Engineering Department, 61080 Trabzon, Turkey
[2] Gümüşhane University, Civil Engineering Department, 29000 Gümüşhane, Turkey
[*][E-mail: mkankal@ktu.edu.tr; mkankal06@gmail.com]

Received 9 December 2010; revised 29 March 2011

Present study consists the growth of a bar profile caused by cross-shore sediment transport. This is especially on growth of bar volume (V) toward equilibrium bar volume (V_{eq}). Three analysis methods being a power and linear regression analysis (PRA and LRA) and an Artificial Neural Network (ANN) analysis were performed to determine empirical temporal rate coefficient (α). Forty-two experimental data were used for training set and the rest of the experimental data were used for testing set in the ANN analysis. As the results of analyses, the smallest average relative and root mean square error (RMSE) computed for the ANN methods are 7.578% and 0.029, respectively. It has been obtained that the ANN analysis, which is used for determination of α coefficient, gives reasonable results. Finally, bar volumes were calculated by means of computed α values and compared with the results of experimental data.

[**Keywords:** Coastal profiles; Artificial neural network; Temporal variation; Bar volume; Sediment Transport]

Introduction

Cross-shore sediment transport is relevant to a number of coastal engineering problems[1]. A general literature review including the studies carried out previously on this subject is summarized as follows: Larson and Kraus[2] studied erosion and accretion profiles proposing equations for bar parameters of beach profiles using experimental data. Work and Dean[3] introduced an equilibrium profile solution for the situation where a cross-shore profiles features linear or exponentially varying representative grain size across a profile. Silvester and Hsu[4] analyzed beach profile parameters by non-linear regression techniques using various experimental data obtained from previous works and proposed equations for the bar parameters. Hsu[5] performed experimental and theoretical studies to determine the geometry of offshore bars and suggested some equations for bar parameters. Ruessink *et al.*[6] made an attempt to determine long time variations of bar crest position in a beach profile using the remote sensing method. Günaydın and Kabdaşlı[7, 8] studied the characteristics of coastal erosion and bars using a physical model in which the mean diameter of particles of 0.35 and the beach slope of 1/5 under regular and irregular wave conditions. Their results show that the wave types, whether regular or irregular, were not effective in describing the geometric characteristics of coastal erosion. Kömürcü *et al.*[9] investigated bar parameters of beach profiles by using a physical model and obtained dimensional and non-dimensional equations by regression analyses in which the experimental results are used. The physical model results were also evaluated by the genetic algorithms (GAs). The results of this research show that estimates of bar parameters by the GAs give a better estimation performance with respect to other conventional methods[10]. Kankal[11,] by taking in the consideration of wave height and period, bed slope and sediment diameter, studied the temporal variation of cross-shore sediment transport in a physical model and determined temporal rate coefficients by regression analysis. The results of this study show that wave height is the most important parameter on temporal rate coefficients.

Recently, the application of ANN technique in ocean and coastal engineering has increased rapidly. There are many studies that ANN applications focused on various parameters; such as wave height[12–20], sea levels[21–23,] and tidal levels and timings of high and low water[24–28.] Whereas there are a few ANN applications dealing with sediment transport[29, 30]. Present study is an attempt to develop an appropriate model for estimation of α coefficient, which is used to determine the temporal variation of bar volume, by training with

*Corresponding author: Murat Kankal

experimental data including initial bed slope (m), grain size (d_{50}), wave period (T), and wave height (H_0). For this matter, three different analyses methods being PRA, LRA, and ANN techniques are performed and the results obtained from these analyses methods are compared.

Materials and Methods

Equilibrium Profile

A fundamental assumption of beach profile change is the existence of an equilibrium profile to which a beach will tend to achieve equilibrium if exposed to constant wave conditions for a sufficiently long time. The idea is that the beach profile in its equilibrium state dissipates incident wave energy without significant net change in shape[31]. If an equilibrium profile did not exist, the beach would continue either to erode or accrete indefinitely, if exposed to the same wave conditions and with no restrictions in the sand supply. A great difference between initial profile and equilibrium profile for a specific wave climate and grain size implies that a large amount of sand must be redistributed in the process of reaching equilibrium[32].

In considerations of cross-shore sediment transport, it is useful to first examine the case of equilibrium in which there is no net cross-shore sediment transport[1]. As a bar grows, it moves offshore and increases in volume to approach an equilibrium size (Fig. 1). The equilibrium bar volume, however, is not entirely reached in most cases. In such cases, an objective method for determining equilibrium bar volume becomes very important.

In fact, at a micro scale level, the concept of an equilibrium profile is an idealization that cannot be fully achieved in practice, since waves, water level, water temperature, and other conditions cannot be held perfectly fixed. Nevertheless, at a macro scale level, it has been demonstrated that an equilibrium profile can be approached, in which no significant systematic net sand transport occurs, although small perturbations still remain. From a practical point of view, it is of great significance if a natural beach of a certain representative grain size has a preferred shape under a given wave climate. A greater difference between initial profile for a specific wave climate and grain size implies that a greater amount of sand must be redistributed in the process of reaching equilibrium[2].

Cross-shore sediment transport models can be classified into two groups; open and closed loop models. Closed loop cross-shore sediment transport models are based on equilibrium beach profile concepts and assume that, a profile will eventually achieve equilibrium if exposed to the same conditions for a long time. Cross-shore transport is caused by deviations of a beach profile from the equilibrium. Several numerical models have been developed according to equilibrium beach profile concepts.

The beach profile characterization which has been the most widespread use throughout coastal engineering application is that which was originated by Bruun[33] in 1954 and supported on a theoretical basis by Dean[34, 35] and is called the $x^{2/3}$ model because of fallowing relationship:

$$h = Ax^{2/3} \qquad \ldots (1)$$

where h is a still-water depth at a horizontal distance (x) from the shoreline (m), A is a dimensionless shape parameter called the “proportionality coefficient” and x is distance from the shoreline (m). The “proportionality coefficient” (A) can be quantified based upon either mean sediment grain-size diameter (Eq. 2) or mean sediment settling velocity (Eq. 3):

$$A=0.21D^{0.48} \qquad \ldots (2)$$

where D is a mean grain size (mm).

$$A=0.067w^{0.44} \qquad \ldots (3)$$

where w is a sediment fall velocity (cm/s)[36].

As a bar moves offshore, it increases in volume to approach an equilibrium size. Since equilibrium bar

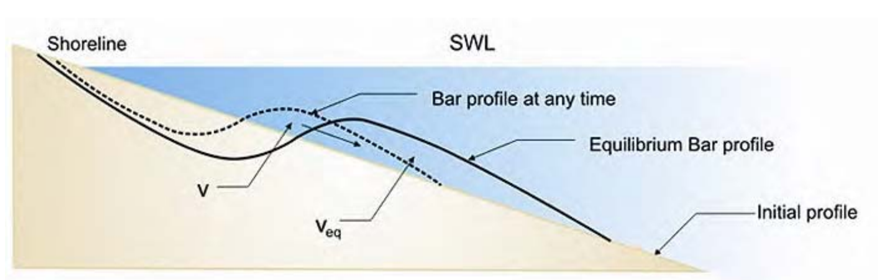

Fig. 1—The equilibrium profile

volume was not entirely reached in some cases, and in order to obtain an objective method for determining equilibrium bar volume, a simple expression of exponential type was least-square fitted to the data for each case. Generally, an expression of exponential type is employed in growth problems where an equilibrium state exists [2]. In this expression, the bar volume (V) is assumed to grow toward the equilibrium volume (V_{eq}) according to

$$V=V_{eq}\,(1-e^{-\alpha t}) \qquad \ldots (4)$$

where t and α are time and an empirical temporal rate coefficient, respectively. α value controls the speed at which equilibrium bar volume is attained; a large α value produces a rapid response toward equilibrium. Several experimental studies have showed that equilibrium bar volume is most closely related to deepwater wave height, sand grain size (or fall speed), and initial beach slope. Various studies were also performed to relate α to some wave, sediment, and beach parameters[2].

ANN Approach

ANNs are human attempts to simulate and understand what goes on in nervous system, with the hope of capturing some of the power of these biological systems. ANNs are inspired by biological systems with large number of neurons which collectively perform tasks that even the largest computers have not been able to match.

The function of artificial neurons is similar to that of real neurons; they are able to communicate by sending signals to each other over a large number of biased or weighted connections. Each of these neurons has an associated transfer function which describes how the weighted sum of its input is converted to an output (Fig. 2).

Different types of ANNs have evolved based on the neuron arrangement, their connections and training paradigm used. Among the various type of ANNs, the multi-layer perceptron (MLP) trained with back propagation algorithm has been proved to be most useful in engineering applications. Backpropagation is a systematic method for training multi-layer perceptron.

The multi-layer perceptron network comprises an input layer, an output layer and a number of hidden layers (Fig. 3). The presence of hidden layers allows the network to present and compute more complicated associations between patterns. Basic methodology of ANNs consists of two processes; network training and testing.

The connection weights of the ANN are adjusted through the training process, while training effect is referred to as supervised learning. The training of ANNs usually involves modifying connection weights by means of learning rule. The learning process is done by giving weights and biases computed from a set training data or by adjusting weights according to a certain condition. Then other testing data are used to check the generalization. The purpose of the bias input of a back propagation network is to stabilize the origin of activation function to provide better learning[37]. The initial weights and biases are commonly assigned randomly. As input data are passed through hidden layers, sigmoidal activation function is generally used. During the training procedure, the data are selected uniformly. A specific pass is completed when all data sets have been processed. Generally, several passes are required to attain a desired level of estimation accuracy. Training actually means for each input pattern and then compares it with the correct output. The total error based on the squared difference between predicted and actual output is computed for the whole training set. The adjustment of the corrections weights has been carried out using the standard error back propagation algorithm, which minimizes the total error (E) with the gradient decent method[38, 39].

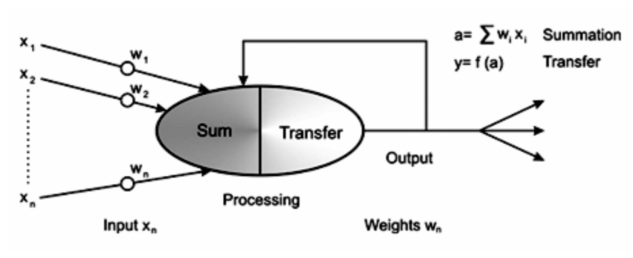

Fig. 2—Artifical neuron

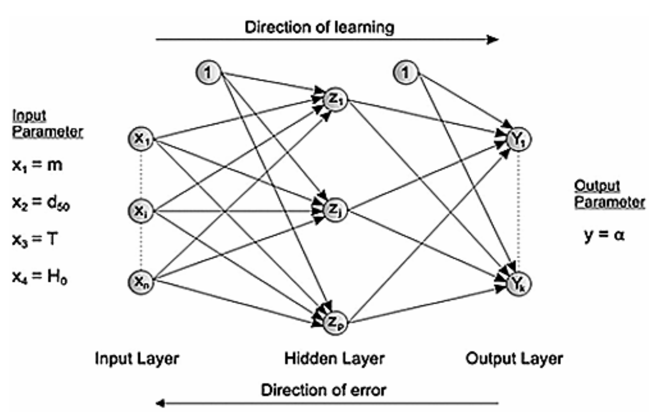

Fig. 3—The architecture of back-propagation network model

Weight uptade formula in the back-propagation algorithm is given as follows:

$$w_{j(l-1)^{h_L}}(t+1)=w_{j(L-1)^{h_L}}(t)+\gamma\delta^k_{h_L}x^k_{j(L-1)}+\eta[w_{j(L-1)^{h_L}}(t)-w_{j(L-1)^{h_L}}(t-1)] \quad \ldots (5)$$

where γ is learning rate, η is momentum parameter, L is layer number and x^k is output vector.

The total sum squared error is calculated as follows:

$$\left\langle E^k \right\rangle = \left\langle \frac{1}{2}\sum_{i_0=1}^{M}(y^k_{i_0}-x^k_{i_0})^2 \right\rangle \quad \ldots (6)$$

where y^k is a desired output vector [40]. The foregoing algorithm used in this study updates the weights after an epoch is presented. Epoch is one cycle through the entire set of training patterns.

Experimental Study

Wave flume and measuring method

The experiments have been conducted in a wave flume with 30 m length, 1.4 m width, and 1.2 m depth. The wave generator is located at the beginning of the flume, which has a sandy beach model at the end (Fig. 4). The wave characteristics were measured using three wave gauges and recording units. In each case, reflection coefficients in the experiments were estimated to be less than 7.1% (actually it changes between 2.2% and 7.1%). The flume was divided into 70 longitudinal sections and each section was divided into three horizontal measuring points (i.e., three depths were measured and averaged in a section) and 210 total points were measured during an experiment (Fig. 5). A uniform measurement grid of 20 × 20 cm was surveyed within the mesh. At each point and time of interest, sand elevations above the basin floor were simply measured [9, 10, 41].

Experimental variables

The experiments have been performed to investigate the variation in the coastal profile under different scenarios. The experimental studies were prepared using Froude's model technique under undistorted conditions. The scale of the model was chosen to be 1/25 by taking into account the size of the wave flume. In all tests, regular (monochromatic) waves were used. Wave conditions were chosen to be between a maximum and minimum to originate the erosion profile, as would be in nature, in order to examine the considered parameters. The deepwater wave heights (H_0) were chosen as 6.5, 11.5, 16, 20, 23, 26, and 30 cm for a 1.46 s wave period

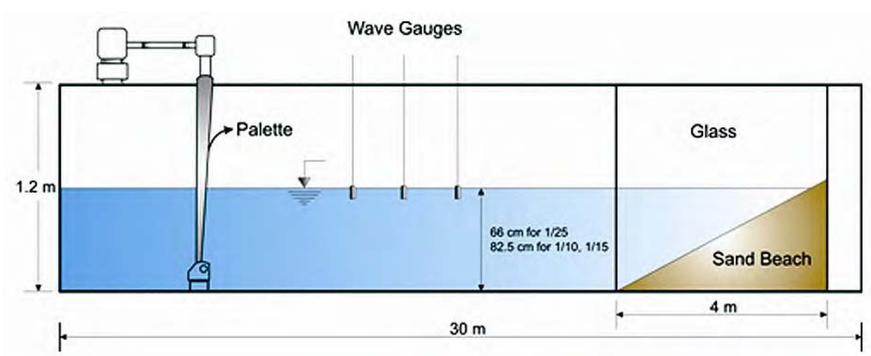

Fig 4—The regular wave flume[9, 10, 41]

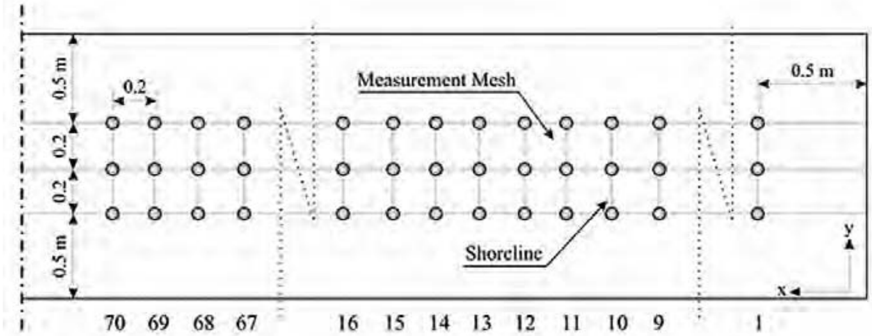

Fig 5—Measurement mesh in the wave flume[9, 10, 41]

(T), and also 11.5, 16, and 20 cm for a 2.03 s wave period. The initial bed slopes (m = tan b) were fixed as 1/10, 1/15, and 1/25, representing slopes in nature and to make lab conditions easy.

Four different granular materials with the mean diameters (d_{50}) 0.18, 0.26, 0.33, and 0.40 mm were used, and the specific gravity of the materials was 2.55 t/m^3. The uniformity of materials is another important aspect for sediment transport. As materials uniformly distributed around the same diameter closely move each other, the determination of diameters in these materials is therefore strictly considered.

There is also a relationship between experimental time and erosion parameters. The experimental time was determined during a preliminary test for each beach slope to find the time for the erosion profile to reach equilibrium. This duration was determined by several criteria: maintain the initial erosion point, equilibrium point and final bar point, decrease the total quantity of moving material to below a certain ratio, and move materials with the same slope; the experiment time was preferred 12h for 1/10 beach slope, while it was selected 14 h for 1/15 and 1/25 beach slopes. All details about the independent parameters mentioned here were listed in Table 1[9, 10, 41].

Analysis of the Experimental Results

Calculation of α values

α Values in Eq. (4) were calculated by using the experimental results. During each experiment, time (t) and the corresponding bar volume (V) values with two hours intervals (Δt=2 hours) were measured. At the end of the experiment (after 12 to 14 hours from the beginning of the experiment), the equilibrium volume (V_{eq}) was also measured. Then, inserting t, V and V_{eq} values in Eq. (4), α values were calculated for each experiment. Total number of α values was $\sum t/\Delta t$, where $\sum t$ is total duration of the experiment (12 to 14 hours).

Since all of the V values did not precisely fit to Eq. (4), some scattering was observed among α values for each experiment. Therefore, it was necessary to find the best fitted α value for the related experiment. A computer programme, which carried

Table 1—Wave and erosion parameters in the test [9, 10, 41]

Test No	m	d_{50} (m)	T (s)	H_0 (m)	Test No	m	d_{50} (m)	T (s)	H_0 (m)
1	0.1000	0.00018	1.46	0.065	27	0.0667	0.00018	2.03	0.200
2	0.1000	0.00018	1.46	0.115	28	0.0667	0.00026	1.46	0.065
3	0.1000	0.00018	1.46	0.200	29	0.0667	0.00026	1.46	0.115
4	0.1000	0.00018	1.46	0.230	30	0.0667	0.00026	1.46	0.200
5	0.1000	0.00018	1.46	0.260	31	0.0667	0.00026	1.46	0.230
6	0.1000	0.00018	1.46	0.300	32	0.0667	0.00026	1.46	0.300
7	0.1000	0.00018	2.03	0.115	33	0.0667	0.00026	2.03	0.200
8	0.1000	0.00018	2.03	0.160	34	0.0667	0.00033	1.46	0.115
9	0.1000	0.00018	2.03	0.200	35	0.0667	0.00033	1.46	0.200
10	0.1000	0.00026	1.46	0.160	36	0.0667	0.00033	1.46	0.300
11	0.1000	0.00026	1.46	0.230	37	0.0667	0.00033	2.03	0.115
12	0.1000	0.00026	1.46	0.300	38	0.0667	0.00033	2.03	0.160
13	0.1000	0.00026	2.03	0.115	39	0.0667	0.00033	2.03	0.200
14	0.1000	0.00026	2.03	0.160	40	0.0667	0.00040	1.46	0.160
15	0.1000	0.00033	1.46	0.115	41	0.0667	0.00040	1.46	0.260
16	0.1000	0.00033	1.46	0.160	42	0.0667	0.00040	1.46	0.300
17	0.1000	0.00033	1.46	0.200	43	0.0400	0.00018	1.46	0.115
18	0.1000	0.00033	1.46	0.230	44	0.0400	0.00018	1.46	0.160
19	0.1000	0.00033	2.03	0.115	45	0.0400	0.00018	2.03	0.115
20	0.1000	0.00040	1.46	0.160	46	0.0400	0.00018	2.03	0.160
21	0.1000	0.00040	1.46	0.230	47	0.0400	0.00026	1.46	0.115
22	0.1000	0.00040	1.46	0.300	48	0.0400	0.00026	1.46	0.160
23	0.1000	0.00040	2.03	0.200	49	0.0400	0.00026	2.03	0.115
24	0.0667	0.00018	1.46	0.065	50	0.0400	0.00033	1.46	0.115
25	0.0667	0.00018	1.46	0.115	51	0.0400	0.00033	1.46	0.160
26	0.0667	0.00018	1.46	0.300	52	0.0400	0.00033	2.03	0.160

Table 2—Regression coefficients and R^2 values for PRA and LRA

Equation type	a_1	a_2	a_3	a_4	c	R^2
PRA	0.0029	-0.3009	0.0299	0.8136	0.0874	0.560
LRA	0.1589	-211.7670	0.0408	1.2824	0.0148	0.568

out a least-square analysis among the measured α values, was used to calculate the best fitted α. Totally fifty-two α values were calculated for all of the fifty-two experiments.

Regression analyses

Two equation types were determined in regression analyses, power (PRA) and linear (LRA). These functions are given respectively as follows:

$$y = c\, x_1^{a_1} x_2^{a_2} x_3^{a_3} x_4^{a_4} \quad \ldots (7)$$

$$y = a_1x_1 + a_2x_2 + a_3x_3 + a_4x_4 + c \quad \ldots (8)$$

where y is α coefficient; a_1-a_4 and c are regression coefficients; x_1 is m; x_2 is d_{50}; x_3 is T and; x_4 is H_0. Using a least-square method, the regression coefficients were estimated. The regression coefficients and R^2 values are given in Table 2.

Construction, teaching and testing of artificial neural network

The main objective of this section is to develop an appropriate ANN model for estimation of α coefficient by training with experimental data including m, $d_{50,}$ T and H_0. It is important to choose the proper network size. If the network is too small, it may not be able to represent the system adequately. On the other hand, if the network is too big, it becomes over trained and may provide erroneous results for untrained patterns. In general, it is not straightforward to determine the best size of the networks for a given system. As shown in Fig. 3, a three layer network is selected for the present study. Each layer is connected to the next but no connections exist between neurons on the same level. The number of neurons in the first and third layers, which contain input and output data respectively, is predetermined and depends on the problem at hand. There are four nodes in the input layer corresponding to the four variables and α coefficient (y) is in the output layer. The variables in the input layers are the following: x_1 is m; x_2 is d_{50}; x_3 is T and; x_4 is H_0.

They are split into the training and testing patterns of the numbers 42 and 10, respectively. Input values of the training and testing set (test no 2, 5, 9, 17, 28, 32, 34, 38, 41, and 48) are given in Table 1.

Table 3—Parameters used for different ANN structures

Number of hidden layer unit	Learning rate (γ)	Momentum (η)
5	0.10	0.10
10	0.25	0.25
15	0.50	0.50
20	0.75	0.75
	1.00	1.00

Data preprocessing is also known as data normalization. Raw data needs to be preprocessed into a range that can be accepted by the network. Hyperbolic tangent sigmoid (input layer → hidden layer) and logistic sigmoid (hidden layer → output layer) transfer functions are used within the network. Scaling of the inputs to the range [0, 1] greatly improves the learning speed. Therefore, each group of input and output values are normalized into range [0.1, 0.9] as,

$$\text{Normalised value} = \left[\frac{\text{Raw vlaue-Minimum value}}{\text{Maximum valu-Minimum value}}\right] \times (0.9-0.1)+0.1 \quad \ldots (9)$$

The definition of network size is a compromise between generalization and convergence. Convergence is the capacity of the network to learn the pattern on the training set and generalization is the capacity to respond correctly to new patterns. The idea is to implement the smallest network possible, so it is able to learn all patterns and at the same time provide good generalization. As for the number of hidden layer, it is well said that one hidden layer is sufficient for most usual applications[42], thus only one hidden layer is used in this study. Determining the number of nodes to include in the hidden layer is not an exact science, so network is tested for different number of hidden layer nodes. Parameters used to find optimum ANN structures are given in Table 3. During the training process, all the training patterns are introduced to the network and corresponding outputs are obtained. Then the network error (E) is computed according to Eq. (6) and the increments of generalized weights are computed by Eq. (5). The choice of initial weights will influence the net reaches a global minimum of the error and, if so, how quickly it converges. As mentioned earlier the update of the weight between two units depends on both the derivative of the upper unit's activation function and the activation of the lower unit. For this reason, it is important to avoid choices of initial weights that would make it likely that either activations or derivatives of activations are zero. In this study, the weights are initialized into random values between -0.5 and 0.5, a procedure commonly accepted. Factors γ and η in Eq. (5) also influence the convergence. γ, the learning rate, is the constant of proportionality of the generalized rule. The larger the value is the greater the changes in weights, η the momentum term, is used to smooth out the weight changes to prevent network training from oscillating. Different combinations of selected values of γ and η are tried for good convergence of the neural network (Table 3).

Memorization is a fundamental problem encountered in training of artificial neural network. To prevent this, the training is cut when the network begins to memorize. In this situation, training set error continues to decrease, although testing set error does not change. Because of training of the network is cut before memorizing, error values of the training set may be greater than the testing set in models.

The level of convergence in training is monitored using total sum squired error of training and testing patterns separately. The patterns are presented to each epoch in the same order. After the learning set of data presented to the ANN models, the learning process is stopped when the epochs reached 50000 and epoch number, which gives the minimum total sum squired error of testing set for various ANN alternatives, is determined. Table 4 shows the structures of the ANN which gives the best results.

Results and Discussion

It is found that there is a tradeoff between the performance of a network and time consumed. Generally, the performance of a network is found to increase with the suitable increase in the number of samples, epochs (learning time) and the number of hidden layer nodes. Meanwhile, the increase of these parameters also increases consumed time. It may be said that besides hidden layer nodes, epochs and number of samples, learning rate (γ) and momentum term (η) influence network to provide good generalization too much[43].

In the ANN analysis, the smallest average relative error value in the testing sets are obtained from the network with $\gamma = 0.1$ and $\eta = 1.0$ as 7.578% (Table 4). The maximum relative error of testing data set in this case is 15.519%. Maximum relative error may be reduced if stopping criteria, epoch number, is increased. Besides, conjugate gradient or scaled conjugate gradient methods may be used to reduce maximum relative error instead of generalized delta rule in learning. Different network structures with one or more hidden layers or nodes with different learning rates and momentum terms may also produce smaller error. Relative error is calculated as

$$e_{rel} = \left(\frac{O_{ANN} - O_{real}}{O_{real}}\right) * 100 \qquad \ldots (10)$$

and, the root mean squared error (RMSE) is defined as follows

$$\text{RMSE} = \left[\frac{1}{n}\sum_{i=1}^{n}(O_{NN} - O_{real})^2\right]^{1/2} \qquad \ldots (11)$$

where n is the number of observation and O_{ANN} and O_{real} are the computed and real values, respectively. Testing set is used to evaluate the confidence in the performance of the trained network. Ten testing vectors are used to test the ANN model. Fig. 6 is an expression of the learning results of network, each plus sign standing for a testing vector. Results obtained from regression analysis (LRA and PRA) for the same values are also shown with triangles and crosses in the same figure. The nearer the points gather around the diagonal, the better are the learning results. The relative errors of the points on the diagonal are zero. The maximum relative errors computed for the ANN, LRA and PRA methods are

Table 4—Characteristics of ANN which gives the best results

Number of hidden layer unit	γ	η	Epoch	Train error[a]	Testing error[a]	RMSE for testing set	Max. relative error (%) in testing set	Average relative error (%) of testing set
10	0.10	1.00	27651	0.3180	0.0236	0.029	15.519	7.578

[a] Error values were calculated from Eq. 5

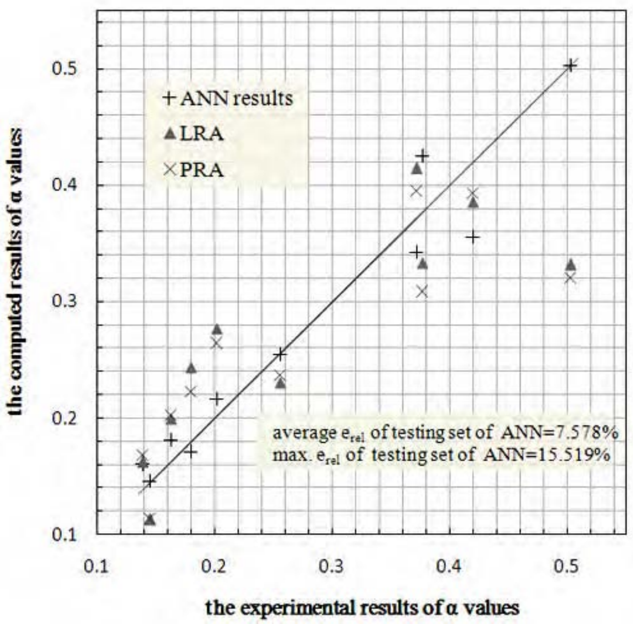

Fig. 6—Comparison of the computed result with the experimental result for the α values

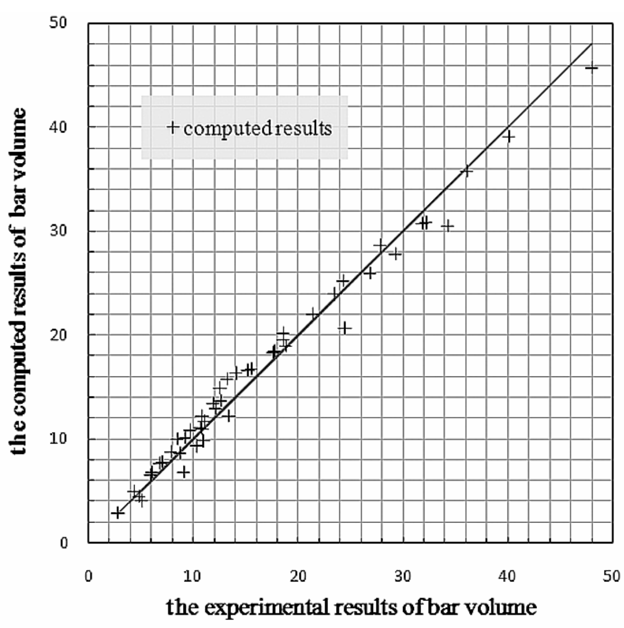

Fig. 7—Comparison of the computed result with the experimental result for the bar (10^{-2} m^3/m)

15.519%, 37.062% and 36.273%, respectively. Their average relative errors are 7.578%, 20.865% and 19.604%, respectively. RMSE values computed for ANN, LRA and PRA methods are 0.029, 0.069 and 0.070, respectively. Thus the ANN method gives significantly better result for the all error values (Table 5).

Table 5—Model results for the testing set

Analysis Method	Ave. e_{rel} (%)	Max. e_{rel} (%)	RMSE
PRA	19.604	36.273	0.070
LRA	20.865	37.062	0.069
ANN	7.578	15.519	0.029

Table 6—Average relative errors for computed values of bar volume

Test No	Average Relative Errors (%)	Test No	Average Relative Errors (%)
2	11.63	32	3.68
5	6.95	34	9.98
9	5.26	38	6.66
17	6.02	41	5.31
28	7.79	48	15.40

For the testing set, bar volumes for each measuring time were calculated by means of Eq. (4) by using α coefficients forecasted with ANN model. Then, computed bar volumes were compared with bar volumes measuring from physical model (Fig. 7). Average relative error values obtained in the result of comparison are given in Table 6. As can be seen from this table, the biggest average relative error value is found as 15.40% for test no 48. Besides, average of computed relative error values for bar volume is 7.87%.

As a consequence, it is shown that ANN analysis, which is used for determination of α coefficient, gives reasonable results. Also, it is understood that bar volume values found by using computed α values are rather suitable.

After training is accomplished, the network becomes able to respond upon unknown input. In this way, the constructed network can be used to recognize and generate patterns given by new inputs. The trained ANN model is used to simulate different values of wave height while the other parameters (m, d_{50} T) remain the same in the test. Table 7 summarized the data, which is entered the constructed ANN network for different values of wave height, and the experimental data used in comparisons. The data was classified as they can be easily analyzed. The data simulated with ANN model was designated as ANN1 – ANN8. In Fig. 8, comparison of the results (α values) obtained from ANN and physical models for each group was given. α value increases with increasing wave height and the simulated ANN model results also supports this.

Table 7—Characteristics of the data simulated with ANN model and the experimental data used in comparison

Group Number	Test No	m	d_{50} (m)	T (s)	H_0 (m)
1	2				0.115
	ANN1	0.1000	0.00018	1.46	0.160
	3				0.200
2	11				0.230
	ANN2	0.1000	0.00026	1.46	0.260
	12				0.300
3	20				0.160
	ANN3	0.1000	0.00040	1.46	0.200
	21				0.230
4	21				0.230
	ANN4	0.1000	0.00040	1.46	0.260
	22				0.300
5	25				0.115
	ANN5	0.0667	0.00018	1.46	0.200
	26				0.300
6	29				0.115
	ANN6	0.0667	0.00026	1.46	0.160
	30				0.200
7	34				0.115
	ANN7	0.0667	0.00033	1.46	0.160
	35				0.200
8	40				0.160
	ANN8	0.0667	0.00040	1.46	0.200
	41				0.260

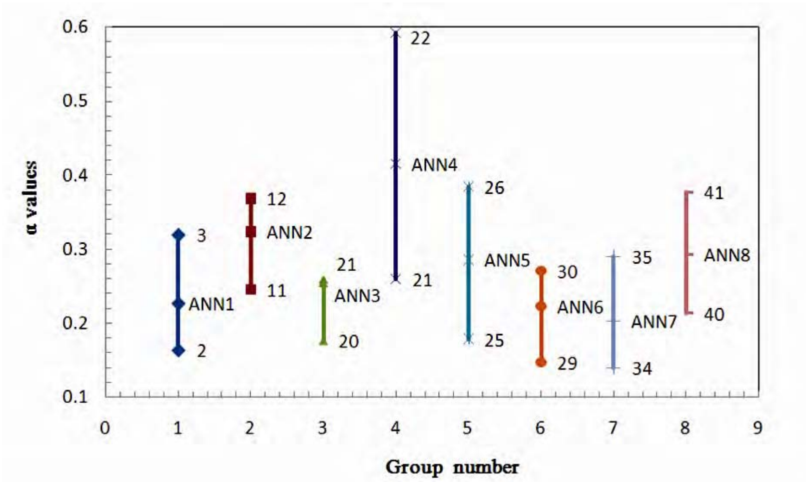

Fig. 8—The change of α values for different values of wave height

Conclusions

In this study, 52 experiments were carried out to determine empirical temporal rate coefficient. Natural beach sand (median size d_{50} = 0.18, 0.26, 0.33, and 0.40 mm and specific gravity of the sand γ_w= 2.55 t/m^3) were used in the experiments. The initial beach slopes were selected 1/10, 1/15, and 1/25. Wave heights were taken 6.5, 11.5, 16, 20, 23, 26, and 30 cm, while the wave periods were 1.46 and 2.03 s.

Three analysis methods, which are the PRA, LRA, and ANN analyses, were performed to determine α coefficient. As the results of analyses, the smallest average relative error and RMSE values for testing set are obtained from ANN methods with 7.578% and 0.029, respectively. ANN analysis, which is used for determination of α coefficient, gives better results than regression analyses. Besides, bar volumes, which are calculated by means of computed α values, were compared with the results of experimental data and, in the result of this, average relative error value is obtained as 7.87%.

The ANN model was also simulated for different values of wave height. In this way, it was determined that α value increases with increasing wave height. As a result, it is shown that the ANN model can effectively predict the α values in spite of wave height.

The use of ANN model for experimental studies has begun recently in coastal and ocean engineering. Since the results of ANN model are found to be satisfactory in this study, the usage of its in coastal and ocean engineering are encouraged and recommended for future studies.

References

1 USACE, *Coastal engineering manual, engineer manual 1110-2-1100, vol. 3*., (US Army Corps of Engineers, Washington, DC) 2002.

2 Larson, H. & Kraus, N.C., *Numerical model for simulating storm-induced beach change (SBEACH), report 1*, (US Army Engineer Waterways Experiment Station, Coastal Engineering Research Center, Mississipi, USA) 1989.

3 Work, P.A. & Dean, R., Effect of varying sediment size on equilibrium beach profiles, Proceedings of Coastal Sediment, (1991) 890-904.

4 Silvester, R. & Hsu, J.R.C., *Coastal stabilization, advanced series on ocean engineering*, (World Scientific Publishing) 1997, pp. 560.

5 Hsu, T.W., Geometric characteristics of storm-beach profiles caused by inclined waves, *Ocean Engineering*, Elsevier, 25(1998) 69-84.

6 Ruessink, B.G., Bell, P.S., Enckevort, I.M.J. & Aarninkhof, S.G.J., Nearshore bar crest location quantified from time-averaged x-band radar images, *Coastal Engineering*, Elsevier, 45(2002) 19-32.

7 Günaydın, K. & Kabdaşlı, M.S., Characteristics of coastal erosion geometry under regular and irregular waves, *Ocean Engineering*, Elsevier, 30(2003) 1579-1593.

8 Günaydın, K. & Kabdaşlı, M.S., Investigation of offshore bar geometry under regular and irregular waves, *Journal of Coastal Research*, 21(2)(2005) 374-382.

9 Kömürcü, M.İ., Özölçer, İ.H., Yüksek, Ö. & Karasu, S., Determination of bar parameters caused by cross-shore sediment movement, *Ocean Engineering*, Elsevier, 34(2006) 685-695.

10 Kömürcü, M.İ., Tutkun, T., Özölçer, İ.H. & Akpınar, A., Estimation of the beach bar parameters using the genetic algorithms, *Applied Mathematics and Computation*, Elsevier, 195(2008) 49-60.

11 Kankal, M., *Temporal Variation of Croos-Shore Sediment Transport*, M.D. Thesis, Karadeniz Technical University Graduate School of Natural and Applied Sciences, Trabzon, Turkey, 2004 (in Turkish).

12 Altunkaynak, A. & Özger, M., Temporal significant wave height estimation from wind speed by Perceptron Kalman filtering, *Ocean Engineering*, Elsevier, 31(2004) 1245-1255.

13 Tolman, H.L., Krasnopolsky, V.M. & Chalikov, D.V., Neural network approximations for non-linear interactions in wind wave spectra: direct mapping for wind seas in deep water, *Ocean Modelling*, Elsevier, 8(2005) 253-278.

14 Rao, L. & Mandal, S., Hindcasting of storm waves using neural network, *Ocean Engineering*, Elsevier, 32(2005) 667-684.

15 Kalra, R., Deo, M.C., Kumar, R. & Agarwal, V.K., RBF network for spatial mapping of wave heights, *Marine Structures*, Elsevier, 18(2005) 35-49.

16 Lee, T.L., Neural network prediction of a storm surge, *Ocean Engineering*, Elsevier, 33(2006) 483-494.

17 Lee, T.L., Prediction of storm surge and surge deviation using a neural network, *Journal of Coastal Research*, 24(4C)(2008) 76-82.

18 Günaydın, K., The estimation of monthly mean significant wave heights by using artificial neural network and regression methods, *Ocean Engineering*, Elsevier, 35(2008) 1406-1415.

19 Malekmohamadi, I., Ghiassi, R. & Yazdanpanah, M.J., Wave hindcasting by coupling numerical model and artificial neural networks, *Ocean Engineering*, Elsevier, 35(2008) 417-425.

20 Naithani, R. & Deo, M.C., Estimation of wave spectral shapes using ANN, *Advances in Engineering Software*, Elsevier, 36(2005) 750-756.

21 Huang, W., Murray, C., Kraus, N. & Rosati, J., Development of a regional neural network for coastal water level prediction, *Ocean Engineering*, Elsevier, 30(2003) 2275-2295.

22 Makarynskyy, O., Makarynska, D., Kuhn, M. & Featherstone, W.E., Predicting sea level variation with artificial neural network at Hillarys boat harbour, western Australia, *Estuarine Coastal and Shelf Science*, Elsevier, 61(2004) 351-360.

23 Sertel, E., Cigizoglu, H.K. & Sanli, D.U., Estimating daily mean sea level heights using artificial neural networks, *Journal of Coastal Research*, 24(3)(2008) 724-734.

24 Lee, T.L. & Jeng, D.S., Application of artificial neural networks in tide forecasting, *Ocean Engineering*, Elsevier, 29(2002) 1003-1022.

25 Lee, T.L., Back-propagation neural network for long-term tidal predictions, *Ocean Engineering*, Elsevier, 31(2002) 225-238.

26 Chang, H.K. & Lin, L.C., Multi-point tidal prediction using artificial neural network with tide-generating force, *Coastal Engineering*, Elsevier, 53(2006) 857-864.

27 Lee, T.L., Makarynskyy, O. & Shao, C.C., A combined harmonic analysis-artificial neural network methodology for tidal predictions, *Journal of Coastal Research*, 23(3) (2007) 764-770.

28 Liang, S.X., Li, M.C. & Sun, Z.C., Prediction models for tidal level including strong meteorologic effects using a neural network, *Ocean Engineering*, Elsevier, 35(2008) 666-675.

29 Pape, L., Ruessink, B.G., Wiering, M.A. & Turner, I.L., Recurrent neural network modeling of nearshore sandbar behavior, *Neural Networks*, Elsevier, 20(2007) 509-518.

30 Singh, A.K., Deo, M.C. & Sanil, V.K., Neural network–genetic programming for sediment transport, *Maritime Engineering*, The Institution of Civil Engineers, London, 160(3)(2007) 113-119.

31 Larson, M., Kraus N.C., & Wise R.A., Equilibrium beach profiles under breaking and non-breaking waves, *Coastal Engineering*, Elsevier, 36(1999) 59-85.

32 Tinh N.X., *Modelling of coastal overwash*, M.D. Thesis, Lund University, Lund Institute of Technology, Lund, Sweden, 2006.

33 Bruun, P., *Coast erosion and the development of beach profiles*, (US Army Beach Erosion Board, Thechnical Memorandum 44) 1954.

34 Dean, R. G., *Equilibrium beach profiles: US Atlantic and Gulf Coast*, (Department of Civil Engineering, Ocean Engineering Technical Report No: 12, University of Delaware, Newark) 1977.

35 Dean, R. G., Equilibrium beach profiles: characteristics and application, *Journal of Coastal Research*, 7(1) (1991) 53-84.

36 Cooper N. J., & Leggett D. J., Beach-profile measurement, theory and analysis: practical guidance and applied case studies, *Water and Environment Journal*, Wiley, 14(2)(2000) 79-88.

37 Taşgetiren, M.F., *Neural networks: multivariate*, (Sakarya University) (http://elektroteknoloji.com/Elektrik_Elektronik/PLC_Sistemleri/Yapay_Sinir_Aglar_Cok_Katmanli.html) 2010.

38 Fausett, L., *Fundamentals of neural networks*, (Prentice-Hall, New Jersy) 1994, pp. 470.

39 Ozsahin, T.S., Birinci, A. & Cakıroğlu, A.O., Prediction of contact lengths between an elastic layer and two elastic circular punches with neural networks, *Structural Engineering and Mechanics*, Techno Press, 18(2004) 441–59.

40 Halıcı, U., *Artificial neural network*, (Lecture notes, Middle East Technical University, Ankara,Turkey)(http://vision1.eee.metu.edu.tr./~halici/543LectureNotes/543index.html.) 2001.

41 Kömürcü, M.I., *Determination of Bar Parameters Caused by Cross-Shore Sediment Movement*, Ph.D. Thesis, Karadeniz Technical University Graduate School of Natural and Applied Sciences, Trabzon, Turkey, 2003 (in Turkish).

42 Kang, J.Y. & Song, J.H., Neural networks applications in determining the fatigue crack opening load, *International Journal Fatigue*, Elsevier, 20(1997) 57-69.

43 Ozsahin, T.S. & Oruc, S., Neural network model for resilient modulus of emulsified asphalt mixtures, *Construction and Building Materials*, Elsevier, 22(2008) 1436-1445.